II-11. DIRECT POWER AND TORQUE CONTROL SCHEME FOR SPACE VECTOR MODULATED AC/DC/AC CONVERTER-FED INDUCTION MOTOR

M. Jasinski, M. P. Kazmierkowski and M. Zelechowski

Warsaw University of Technology, Institute of Control & Industrial Electronics,
ul. Koszykowa 75, 00-662 Warszawa,
mja@isep.pw.edu.pl, mpk@isep.pw.edu.pl,
zelechom@isep.pw.edu.pl WWW: http://www.ee.pw.edu.pl/icg

Abstract. A novel control scheme for PWM rectifier-inverter system is proposed. Fast control strategies such as line voltage Sensorless Virtual Flux (VF) based Direct Power Control with Space Vector Modulator (DPC-SVM) for rectifier and Direct Torque Control with Space Vector Modulator (DTC-SVM) for inverter side are used. These strategies lead to good dynamic and static behaviour of the proposed control system—Direct Power and Torque Control- Space Vector Modulated (DPTSVM). Simulations and experiment results obtained show good performance of the proposed system. Additional power feedforward loop from motor to rectifier control side improved dynamic behaviours of the power flow control. As a result, better input-output energy matching allows decreasing the size of the dc-link capacitor

Introduction

The adjustable speed drives (ASD) with diode rectifier nowadays is the most popular on the marked. Large electrolytic capacitor is used as an energy-storing device to decouple rectifier and the inverter circuits. The capacitors have some drawbacks: low reliability, high size, weight and cost. Hence, reliability of the dc-link capacitor is the major factor limiting the lifetime of the ASD systems [1].

Development of control methods for Pulse Width Modulated (PWM) boost rectifier (active rectifier) was possible thanks to advances in power semiconductors devices and Digital Signal Processors (DSP). Therefore, the Insulated Gate Bipolar Transistors (IGBT) AC/DC/AC converter controlled by PWM is used in motor drive systems (Fig.1). Thanks to active rectifier the dc-link capacitor can be reduced [2]. Farther reduction of the capacitor can be achieved by power feedforward loop from motor side to the control of the PWM rectifier. A lot of works are given attention to reduce the dc-link capacitor. However, a small capacitance leads to a high dc-voltage fluctuation. To avoid this drawback various dc-voltage control schemes have been proposed. Some of them take into account the inverter dynamics

S. Wiak, M. Dems, K. Komęza (eds.), Recent Developments of Electrical Drives, 261–274.

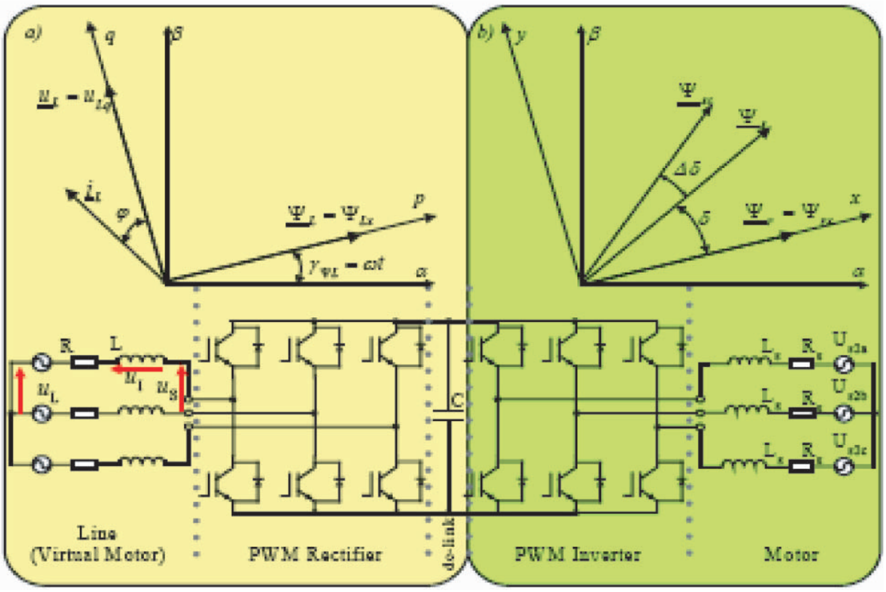

Figure 1. Representation of three-phase PWM rectifier—inverter system; vector diagram and coordinate system for: a) PWM rectifier side b) inverter side.

to improve the PWM rectifier current control by feedback linearization [3] and master-slave [1] manner. Another control methodology proposed a fast dc-link voltage controller which works with dc-voltage and motor variables as inputs [4]. Moreover, various methods of the output power estimation have been discussed in [5].

In the mentioned methods active and reactive powers of the PWM rectifier are indirectly controlled via current control loops. Besides, stator current controllers control the torque and flux of the motor too.

In this paper a line voltage sensorless Virtual Flux (VF) based Direct Power Control with Space Vector Modulator (DPC-SVM) is applied to control of the PWM rectifier.

The inverter with induction motor is controlled via Direct Torque Control with Space Vector Modulator (DTCSVM). Contrary to the scheme proposed in [6], our solution includes not stator flux controller but space vector modulator.

Hence, an AC/DC/AC converter of Fig. 1, is controlled by Sensorless Direct Power and Torque Control-Space Vector Modulated (DPT-SVM) scheme. In comparison to methods that control an active and reactive power, torque and flux in indirect manner the coordinates transformation and decoupling are not required. Moreover, the current control loops are avoided.

In respect of dynamic, of dc-voltage control the power balance between line and motor is very important. Therefore, to improve instantaneous input/output power matching, the additional feedforward power control loop is introduced.

Thanks to better control of the power flow the fluctuation of the dc-link voltages will be decrease. So the size of the dc-link capacitor can be reduced.

Direct power and direct torque control space vector modulated (DPT-SVM) scheme

Direct Power Control (DPC) for PWM rectifier is based on instantaneous control of active p and reactive q power flow from/to the line and to/from active load. In classical approach [7, 8] of DPC there are two power control loops with hysteresis comparators and switching table.

Therefore, the key point of the DPC implementation is sufficiently precise and fast estimation of the instantaneous line powers. The most significant drawbacks of the hysteresis-based DPC are variable switching and high sampling frequency. Introducing a Space Vector Modulator (SVM) in control strategy [9,10] allows to eliminate the both mentioned problems. Moreover, the line voltage sensors can be replaced by Virtual Flux (VF) estimator, which introduces technical and economical advantages to the system (simplification, reliability, galvanic isolation, cost reduction). Such control system is called: Virtual Flux Based Direct Power Control Space Vector Modulated (DPC-SVM) scheme [11]. Summarised, in this method linear PI controllers with Space Vector Modulator replace hysteresis comparators and switching table (Fig. 3).

Similarly like DPC, for the classical Direct Torque Control (DTC) [12], the command stator flux Ψ_{sc} and commanded torque Mec values are compared with the actual stator flux Ψ_s and electromagnetic torque M_{ec} values in hysteresis flux and torque controllers, respectively. Therefore, the well known disadvantages of DTC are: variable switching frequency, ± 1 switching over dc-link voltage U_{dc}, current and torque distortion caused by sector changes as well as high sampling frequency requirement for digital implementation of the hysteresis controllers. All above difficulties can be eliminated when, instead of the switching table, a SVM is used. Hence, the DTC-SVM strategy [13] for control of the inverter/motor part is proposed (Fig. 3).

Simplified mathematical model of the system in stationary α, β coordinates is shown in Fig. 2

DPC-SVM with virtual flux (VF)

A line current i_L is controlled by voltage drop on the input inductance L that placed between two voltage sources (line on the one side and the converter on the other). From Kirchhoff's law the input equations can be wrote:

$$U_L = U_I + U_{s1} \tag{1}$$

where

$$U_I = L\frac{d}{dt}I_L\text{—voltage drop on the inductance}$$

$$U_{sk} = \begin{bmatrix} U_{sk\alpha} \\ U_{sk\beta} \end{bmatrix} = \begin{bmatrix} \frac{2}{3}U_{dc}\left\{DA_k - \frac{1}{2}(D_{Bk} + D_{Ck})\right\} \\ \frac{\sqrt{3}}{3}U_{dc}(D_{Ak} - D_{Bk}) \end{bmatrix} \tag{2}$$

where $k = 1, 2$; 1—for the PWM rectifier, 2—for the PWM inverter.

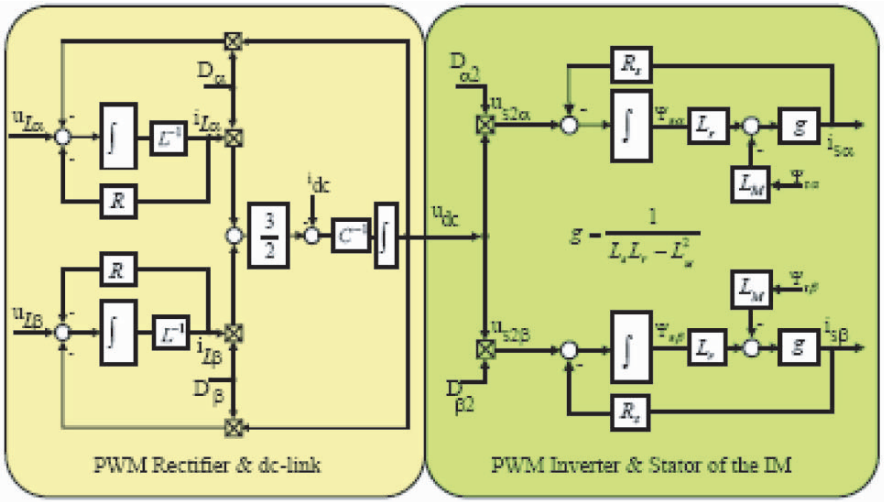

Figure 2. Modified model of AC/DC/AC converter in α, β coordinates.

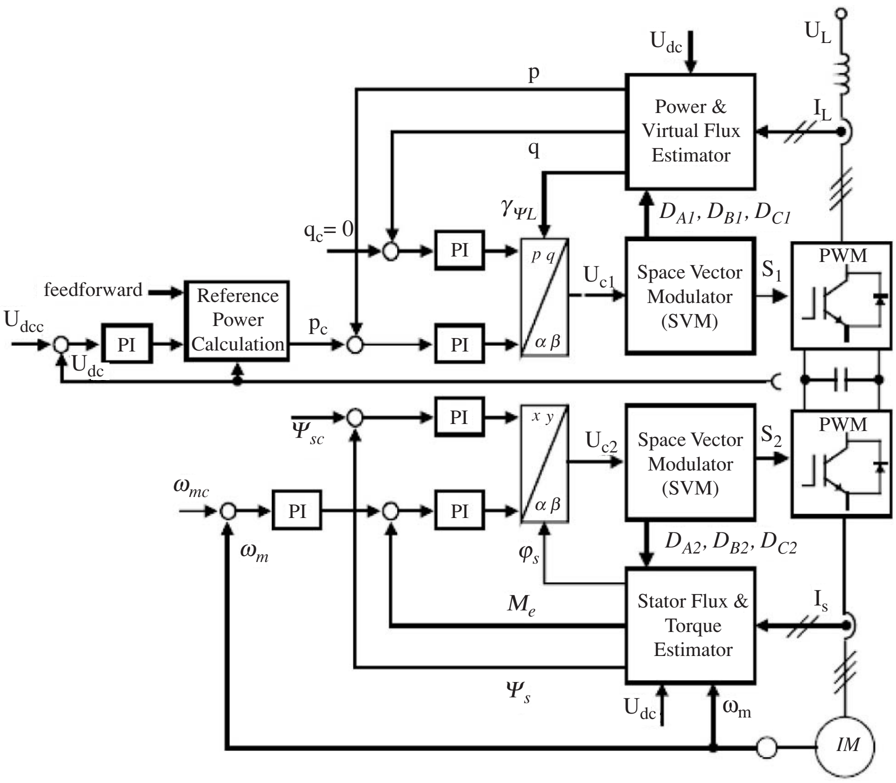

Figure 3. Basic structure of unified direct power and torque control with space vector modulator (DPT- SVM).

Voltage on the input of the converter can be calculated from measured dc-link voltage U_{dc} and duty cycles from PWM rectifier's modulator D_{A1}, D_{B1}, D_{C1} (2). Therefore, proposed DPC-SVM is sensorless line voltage control strategy. Based on assumption that line voltage U_L with input inductances can be related as quantities of virtual AC motor (Fig. 1) and the integration of the line voltage gives Virtual flux linkage of the virtual AC motor, the VF estimator with low pass filter is used.

$$\mathbf{\Psi}_L = \int \left[(\mathbf{U}_S + \mathbf{U}_L) - \frac{1}{T_{f1}} \Psi_L \right] dt \tag{3}$$

The measured line currents and virtual flux linkage obtained from (3) can be used for power calculations [11]. With assumptions that line voltages is sinusoidal and balanced, simple equations are obtained:

$$\begin{aligned} p &= \omega \left(\Psi_{L\alpha} I_{L\beta} - \Psi_{L\beta} I_{L\alpha} \right), \\ q &= \omega \left(\Psi_{L\alpha} I_{L\alpha} + \Psi_{L\beta} I_{L\beta} \right) \end{aligned} \tag{4}$$

Both estimated powers are compared with commanded values p_c, q_c respectively, were q_c is set to zero for fulfilling the unity power factor conditions. The command active power p_c is provided from outer PI dc-link voltage controller. The obtained errors are dc quantities. These signals are delivered to PI controllers that eliminate the steady state error. The PI controllers generate dc-values voltage commands U_{pc}, U_{qc}. After coordinate transformation (5) $pq/\alpha\beta$, $U_{\alpha c}$ and $U_{\beta c}$ are delivered to SVM block, which generates switching signals (Fig. 3).

$$\mathbf{U}_c = \begin{bmatrix} U_{c\alpha} \\ U_{c\beta} \end{bmatrix} = \begin{bmatrix} -U_{qc} \cos \gamma_{\Psi L} - U_{pc} \sin \gamma_{\Psi L} \\ -U_{qc} \cos \gamma_{\Psi L} + U_{pc} \sin \gamma_{\Psi L} \end{bmatrix} \tag{5}$$

DTC-SVM

In control of an induction motor (IM) drive, supplied by a voltage source inverter, there is a possibility to control directly the electromagnetic torque and stator flux linkage by the selection of the optimum inverter switching modes. That control manner is called direct power and torque control (DTC). DTC allows very fast torque responses and flexible control of an IM. To avoid the drawbacks (variable switching frequency, voltage polarity violation) of DTC instead hysteresis controllers and switching table the space vector modulator (SVM) with PI controllers were introduced.

However, it should be noted that DTC with SVM (DTC-SVM) has all advantages of the DTC, and mathematical as well as physical principles are the same. Generally in IM, the instantaneous electromagnetic torque is proportional to the vector product of the stator flux linkage and stator current space vectors (6) in stationary $\alpha\beta$ reference frame.

$$M_e = \frac{1}{2} m_s P_b \mathbf{\Psi}_s \times \mathbf{I}_s \tag{6}$$

where $\Psi_s = \Psi_{sej\varphi s}$—stator flux linkage space vector, $I_s = I_{sej\varphi i}$—stator current space vector φ_s, φ_i—angle of the stator flux linkage space vector and angle of the stator current space vector respectively, in relation to the α axis of the stationary (stator) reference frame.

Therefore, eq. (6) can be converted into (7)

$$M_e = \frac{1}{2} m_s P_b \Psi_s \sin\gamma \tag{7}$$

where $\gamma = \phi_i - \phi_s$—angle between the stator current and stator flux linkage space vectors. Assuming, that modules (amplitudes) of the stator flux linkage is constant, and the angle φ_s is varying quickly, then M_e can be changed with very high dynamics. The rate of change of the increasing M_e is almost proportional to the rate of change $d\varphi_s/dt$ [18]. Summarizing, fast torque control is obtained when stator voltage is on the level, which kept amplitude of the stator flux constant (the voltage drop on stator resistance is neglected), and which rapidly moving the stator flux linkage space vector to demanded position (required by the torque). Therefore, by using appropriate stator voltages the stator flux linkage space vector can be controlled. It is useful to consider another expression for control of the electromagnetic torque (8):

$$M_e = \frac{L_m}{L_r L_\sigma} \Psi_r \Psi_s \sin\delta \tag{8}$$

It base on assumption, that amplitudes of stator and rotor flux linkage are constant. The rotor one because of time constant is large (eg. 0.1 s). Therefore, with this conditions follows from eq. (8) that the Mecan be controlled by changing δ in suitable direction. The δ is called a torque angle and depends on the commanded torque. It should be pointed, that accuracy of the flux calculation is indispensable. That goal can be obtained with a $\mathbf{U}_s$, $\mathbf{I}_s$ ("voltage") model based estimator, with low pass filter (9) or by $\mathbf{I}_s$, γ_m model (10):

$$\boldsymbol{\Psi}_s = \int \left[(\mathbf{U}_{s2} - Rs\mathbf{I}_s) - \frac{1}{TF} \boldsymbol{\Psi}_s \right] dt, \tag{9}$$

or

$$\boldsymbol{\Psi}_s = \frac{L_m}{L_r} \boldsymbol{\Psi}_r + \sigma L_s \mathbf{I}_s \tag{10}$$

Equation (10) ensures better accuracy over the entire frequency range, but it require the angle γ_m of motor shaft position for dq transformation.

Power feedforward control loop

Instantaneous power supplied to an m_s – phase winding can be expressed in terms of complex space vectors as:

$$P = \frac{1}{2} m_s \mathrm{Re}\left[\mathbf{U}_{s2} \mathbf{I}_s^*\right] \tag{11}$$

Taking into consideration the overall power supplied to the stator and rotor windings from (11) can be wrote:

$$P = \frac{1}{2} m_s \left(\mathrm{Re}\left[\mathbf{U}_{s2} \mathbf{I}_s^*\right] + \mathrm{Re}\left[\mathbf{U}_r \mathbf{I}_r^*\right] \right) \tag{12}$$

The losses in resistances can be neglected, thus the internal power is:

$$P_i = P_{mag} + P_e \tag{13}$$

where P_{mag}—is the power stored in the magnetic fields, P_e is the electromagnetic power. From the assumption that only active power is derived from the dc-link to an electric motor and reactive power is derived from the inverter only electromagnetic power can be taken into consideration. In a general way P_e expressed as:

$$P_e = M_e \Omega m \tag{14}$$

where Ω_m—mechanical angular rotor speed, M_e electromagnetic torque.

Hence, active power feedforward can be realized based on Eq. 14. The electromagnetic power is the part of the power supplied to the electrical terminals of an AC motor, that is neither stored nor lost. It corresponds to the voltages induced in rotor windings and to the currents flowing into them [11]. For prediction of the power state of the motor (motoring, regenerating, loaded or unloaded) the commanded values of the electromagnetic torque and mechanical speed can be taken:

$$P_{ec} = M_{ec} \Omega_{mc} \tag{15}$$

Such calculated power can be simply added to the referenced active power of the PWM rectifier. To fulfil the stability conditions of the system the T_w delay should be introduced:

$$P_e = \frac{1}{1 + T_w s} P_{ec} \tag{16}$$

where T_w—time constant of the M_e dynamics.

Thanks to the predictive abilities of motor power feedforward loop a better dc-link voltage stabilization can be obtained. Also, fluctuations of dc-voltages may be reduced.

Dc-link capacitor design

In AC/DC/AC converter with diode rectifier there is no control of the dc-link voltage in particular during transients (Fig. 10). So that, the size of the capacitor should be grater than in a converter with PWM rectifier. A dc-link voltage control accuracy depends on the time constant of the dclink voltage controller. This time constants can be reduced by additional power feedforward control loop.

Having the maximum allowed dc-link voltage fluctuations ΔUdc, the required capacity can be calculated as :

$$C_{PWMm} = P_{out} \frac{\sqrt{2} + \sqrt{3} U_{LLrms} / U_{DC}}{2\sqrt{3} f_s U_{LLrms} \Delta U_{DC}} \tag{17}$$

where P_{out}—rated output power, U_{LLrms}—line to line voltage, f_s—sampling frequency.

Moreover, the general capacitor life time is:

$$L = L_B \times f\,(T_M - T_C) \times f_1\,(U_{dc}) \tag{18}$$

where, L is the life estimate in hours, L_B is the base life elevated maximum temperature T_M, T_C is the actual core temperature and U_{dc} is the applied dc-voltage. The voltage multiplier f_1 at higher stress level may reduce the life of the capacitor [14]. Therefore, the stabilization of the dc-voltage at the required level is important.

Table 1. Parameters of the model

Sampling and switching frequency	5 kHz
Resistance of reactors R	80 mΩ
Inductance of reactors L	10 mH
DC-link capacitor	470 μF
Phase voltage V	230 RMS
Source voltage frequency	50 Hz
DC-link voltage	560 V

Simulation and experimental results

Proposed approach has been tested using Saber simulations packed software. The main data and parameters of the model are shown in Table 1.

An experimental investigation was conducted on a laboratory setup (Fig. 4). The setup consists of: input inductance, two PWM converter (VLT5005, serially produced by Danfoss with replaced control interfaces) controlled by dSPACE DS1103 and induction motor set. The computer is used for software development and process visualization.

Converters, motor and input inductance parameters are shown in Table 2.

In below figures are shown different states of the DPTSVM operation. In Fig. 5a and Fig. 6a the system operates in motoring mode, with power factor near to unity (the current is in phase with the line voltage) and almost sinusoidal waveform of the line current (low Total Harmonic Distortion – THD factor).

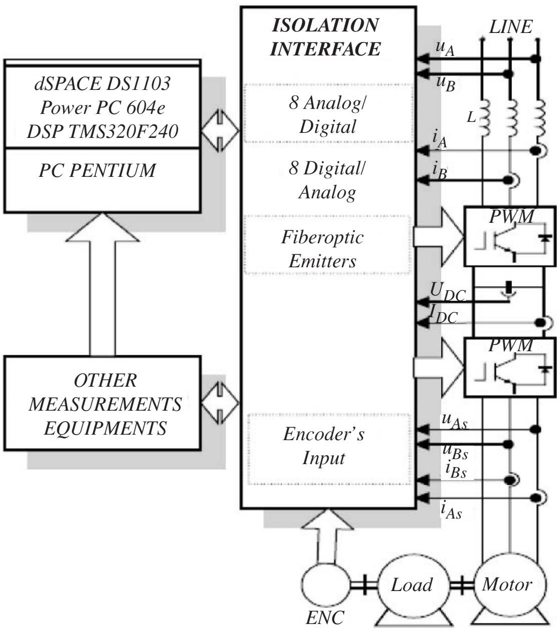

Figure 4. Laboratory setup.

Table 2. Main parameters of the laboratory setup

AC motor	
Stator winding resistance	1.85 Ω
Rotor winding resistance	1.84 Ω
Stator inductance	170 mH
Rotor inductance	170 mH
Mutual inductance	160 mH
Number of pole pairs	2
Moment of inertia	0.019 kgm^2
Phase voltage	230 V(rms)
Phase current I	6.9 A(rms)
Nominal torque MN	20 Nm
Base speed ω_b:	1415 rpm
Input inductance	
Resistance of reactors R	100 mΩ
Inductance of reactors L	10 mH
VLT5005 Converters	
Sampling and switching frequency	5 kHz
DC-link capacitor	470 μF
Nominal power P_N	5,5 kVA
Measurement conditions	
Phase voltage V	150 RMS
Source voltage frequency	50 Hz
DC-link voltage	560 V

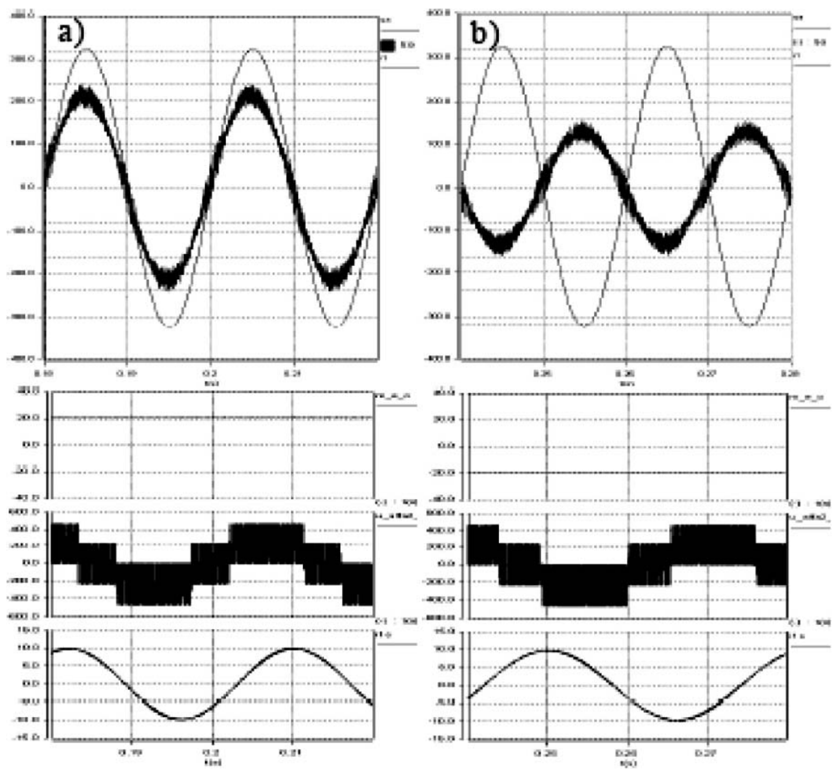

Figure 5. Steady state from the top: i_L—line current 2A/div, U_L—line voltage, M_e electromagnetic torque, $U_{s\alpha}$ component of stator voltage, $i_{s\alpha}$—stator current; a) motoring mode, b) regenerating mode.

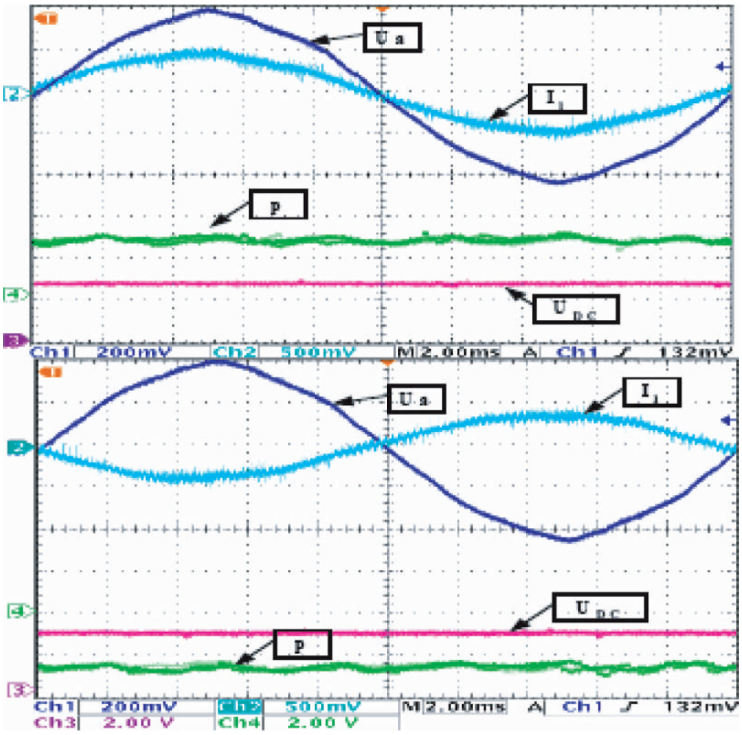

Figure 6. Experimental results—steady state. From the top: line voltage 100 V/div, line current 5 A/div, active power, dc-link voltage, a) for acceleration, b) for regeneration mode.

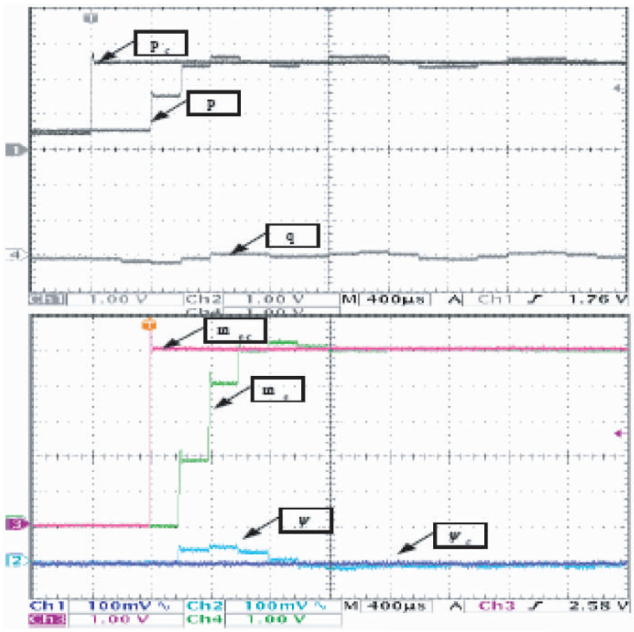

Figure 7. Experimental results. Small signal behaviour of the: a) power control loop ($p_c = 0.1 \rightarrow 0.5$ PN, p—actual active power, q—reactive power; b) torque control loop ($M_{ec} = 0 \rightarrow 1$ $\mathrm{M_N}$), M_e—actual electromagnetic torque, commanded and actual stator flux.

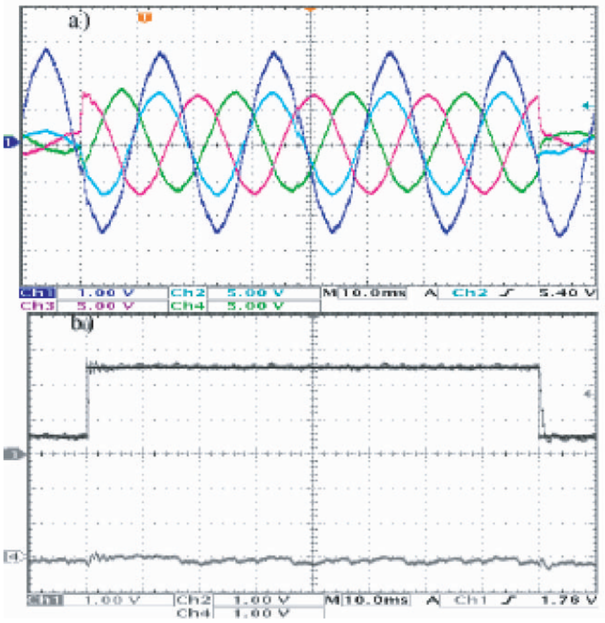

Figure 8. Experimental results. Transient in commanded active power (300–1300 W) a) ch1—line voltage, ch2,3,4—line currents, b) from the top: commanded active power, active power, reactive power.

Oscillograms of Fig. 5b and Fig. 6b illustrates operation of an AC/DC/AC converter in regenerating mode (as a transmitter of the energy from the motor to the line). Note that current is shifted by 180 degree in respect to the line voltage. In Fig. 7 experimental waveforms of the small signal test a) commanded active power and b) electromagnetic torque are presented. Power tracking performance of the PWM rectifier in back-to-back converter is shown in Fig. 8. In Fig. 9 and Fig. 10 are shown the responses to step change of the commanded electromagnetic torque from –5 do 5 Nm. That test was conduced for ac/dc/ac converter with diode rectifier (Fig. 9) as well as for back-to-back converter (Fig. 10). The behaviour of the dc-link voltage can be observed. From Fig. 9a it can be seen that the overshoot in dc-link voltage is significantly bigger then for back-to-back converter (Fig. 10a).

CONCLUSION

Virtual Flux Based Direct Power Control with Space Vector Modulator (DPC-SVM) and Direct Torque Control with Space Vector Modulator (DTC-SVM) are applied to a PWM AC/DC/AC converter. The power of the PWM rectifier and torque of the induction motor is controlled in direct manner. It means that control system operates with end-user quantities. Hence, obtained Direct Power and Torque Control- Space Vector Modulated (DPT-SVM).

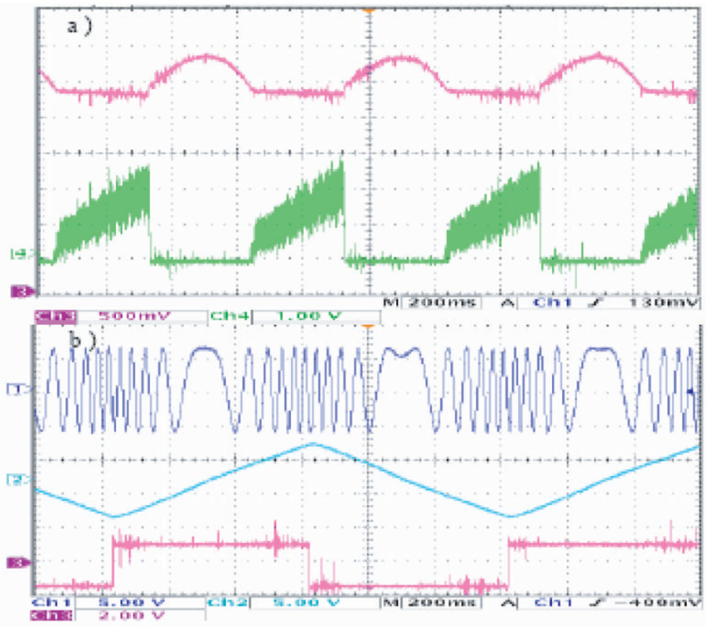

Figure 9. Experimental results with diode rectifier. Transients to commanded torque changes (-5 to 5 Nm). From the top: a) dc-link voltage 100 V/div, active power at the input of the ac/dc/ac converter b) stator current, mechanical speed, electromagnetic torque.

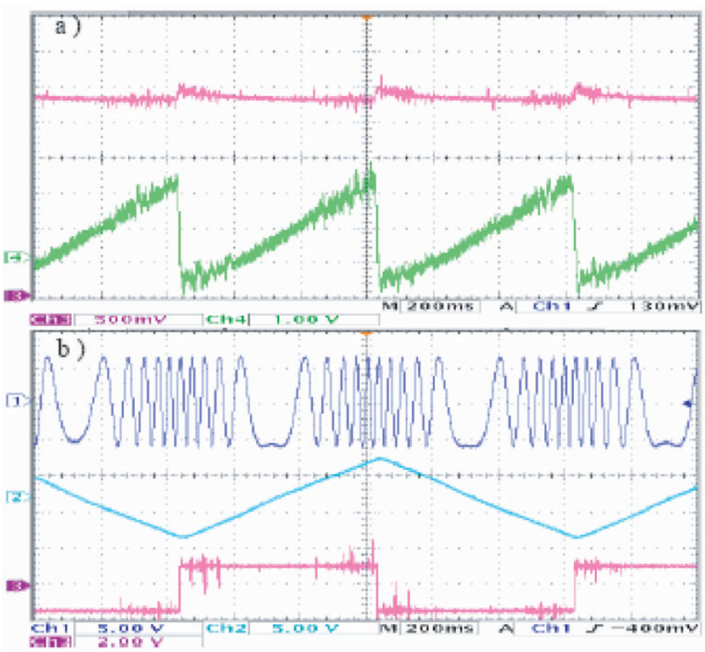

Figure 10. Experimental oscillograms with PWM rectifier. Transients to commanded torque changes (-5 to 5 Nm) From the top: a) dc-link voltage 100 V/div, active power at the input of the ac/dc/ac converter b) stator current, mechanical speed, electromagnetic torque.

Moreover, additional power feedforward control loop was implemented and tested. Proposed control system assures:

- four quadrant operation (energy saving),
- good stabilization of the dc-voltage (allows to reduce a dc-link capacitor),
- constant switching frequency,
- almost sinusoidal line current (low THD) for ideal and distorted line voltage,
- noise resistant power estimation algorithm,
- high dynamics of power and torque control,
- low motor current and torque ripple

Power feedforward loop from the motor side to the PWM rectifier improved control dynamics of the dc-link voltage. It allows fulfilling power matching conditions under transient for PWM rectifier and inverter/motor system.

References

[1] H. Hur, J. Jung, K. Nam, "A Fast Dynamics DC-link Power-Balancing Scheme for a PWM Converter-Inverter System". IEEE Trans. on Ind. Elect., vol. 48, No. 4, August 2001, pp. 794–803.

[2] L. Malesani, L. Rossetto, P. Tenti and P. Tomasin, "AC/DC/AC Power Converter with Reduced Energy Storage in the DC Link," IEEE Trans. on Ind. Appl., vol. 31, No. 2, March/April 1995, pp. 287–292.

[3] J. Jung, S. Lim, and K. Nam, "A Feedback Linearizing Control Scheme for a PWM Converter-Inverter Having a Very Small DClink Capacitor," IEEE Tran. on Ind. App., vol. 35, No. 5, September/October 1999, pp. 1124–1131.

[4] J. S. Kim and S. K. Sul, "New control scheme for ac–dc–ac converter without dc link electrolytic capacitor," in Proc. of the IEEE PESC'93, 1993, pp. 300–306.

[5] R. Uhrin, F. Profumo "Performance Comparison of Output Power Estimators Used in AC/DC/AC Converters," IEEE, 1994, pp. 344–348.

[6] A. Tripathi, A.M. Khambadkone, S.K. Panda, "Space-vector based, constant frequency, direct torque control and dead beat stator flux control of AC machines," Proc. of the IECON '01, Vol.: 2, pp. 1219–1224 vol. 2.

[7] T. Noguchi, H. Tomiki, S. Kondo, I. Takahashi, "Direct Power Control of PWM converter without power-source voltage sensors," IEEE Trans. on Ind. Appl. Vol. 34, No. 3, 1998, pp. 473–479.

[8] T. Ohnishi, "Three-phase PWM converter/inverter by means of instantaneous active and reactive power control," In Proc. of the IEEE-IECON Conf., 1991, pp. 819–824.

[9] J. Holtz "Pulsewidth Modulation for Electronics Power Conversion," In Proc. of The IEEE, vol. 82, no. 8, August 1994, pp.1194–1214.

[10] M. P. Kazmierkowski, R. Krishnan and F. Blaabjerg, Control in Power Electronics, Academic Press, 2002, p. 579.

[11] M. Malinowski, M. Jasinski, M.P. Kazmierkowski, "Simple Direct Power Control of Three-Phase PWM Rectifier Using Space Vector Modulation," in IEEE Trans. on Ind. Elect., vol. 51, No. 2, April 2004, pp. 447–454.

[12] I. Takahashi, and T. Noguchi, "A New Quick-Response and High Efficiency Control Strategy of an Induction Machine," IEEE Trans. on Ind. Appl., vol. IA-22, No. 5, September/October 1986, pp. 820–827.

[13] D. Swierczynski, M.P. Kazmierkowski, "Direct Torque Control of Permanent Magnet Synchronous Motor (PMSM) Using Space Vector Modulation (DTC-SVM),"—Simulation and Experimental Results", IECON 2002, Sevilla, Spain, on-CD.

[14] S.G. Perler, "Deriving Life Multipliers for Electrolytic Capacitors," IEEE PES Newsletter, First Quarter 2004, pp. 11–12.

[15] H. Tajima, and Y. Hori, "Speed Sensorless Field-Oriented Control of the Induction Machine". IEEE Trans. on Ind. Appl., vol. 29, No. 1, 1993, pp. 175–180.

[16] T.G. Habatler, "A space vector-based rectifier regulator for AC/DC/AC converters". IEEE Trans. on Power Electr., vol. 8, February 1993, pp. 30–36.

[17] J.Ch. Liao and S.N. Yen, "A Novel Instantaneous Power Control Strategy and Analytic Model for Integrated Rectifier/Inverter Systems". IEEE Trans. on Power Electr., vol. 15, No. 6, November 2000, pp. 996–1006.

[18] P. Vas, "Sensorless Vector and Direct Torque Control," Oxford University Press, 1998, p. 729.